Size Distribution Measurement of Candle's Soot Nanoparticles by Using Time Resolved Laser Induced Incandescence

A. S. Arabanian, A. Manteghi, F. Fereidouni, and R. Massudi

Laser and Plasma Research Institute, Shahid Beheshti University, Tehran, Iran.

Abstract— **Time resolved laser induced incandescence (LII) technique is used to measure size distribution of soot nanoparticles of candle's flame. Pulsed Nd:YAG laser is used to heat nanoparticles to incandescence temperature and the resulting signal is measured. Mass and energy balance equations are numerically solved to calculate temperature of soot particles in low fluence regime. Assuming Plank black body radiation and lognormal size distribution for soot particles, the intensity of LII signals are calculated. Using Levenberg-Marquart nonlinear regression algorithm and numerical and experimental LII signals, mean particle size and distribution width of soot nanoparticles are obtained.**

KEYWORDS: Laser induced incandescence, heat transfer, size distribution, soot nanoparticle

I. INTRODUCTION

Soot particles generated due to incomplete combustion have major effects on optimum operation of combustion chamber, on human health, and on environment that may cause different diseases, e.g. cancer, Asthma, Bronchitis, and Allergies. To reduce level of such particles in combustion process, that is a requirement in all industries which should fulfill pollution related standards, one should understand production mechanisms of soot particles and to obtain its real time distribution.

It is very important to determine size distribution of such particles because toxic level of soot particles generated by combustion instruments is independent of their total mass but is affected by their size distribution [1].

Destructive and nondestructive methods can be used for size measurement. One drawback of the former methods, e.g. Transmission Electron Microscopy (TEM) and Atomic force Microscopy (AFM), is their low spatial and temporal resolutions and, therefore, they are not appropriate to be used on studying nanoparticles exist in turbulent fluids in engines and other combustion systems[2,3]. On the contrary, nondestructive techniques, which are often optical methods, e.g. Rayleigh scattering and Laser Induced Incandescence (LII), are suitable for turbulent systems.

LII technique is fast, in situ, on line, and repeatable that results to high spatial and temporal resolution and offers precise measuring of different parameters of soot particles, e.g. size distribution, density, soot volume fraction [4]. Furthermore, due to the possibility of using high peak power lasers, the method can be used in turbulent flames and heavy exhaust (without need of dilution).

Size measurement technique using LII was first introduced by Weeks and Duley in 1974 [5]. In 1984, Melton used the same method to calculate size of soot particles and presented a theoretical model to show that decay time of the LII signal is a measure of particle size distribution [6]. Experimental realization of the method was first performed by Will in 1995 [7].

Time Resolved LII (TIRE LII) method was first introduced by Roth and Filippov in 1996 to determine size distribution of particles by measuring their time dependent emission during cooling process after being illuminated by laser pulses [8]. Thereafter, TIRE-LII is used as a powerful method to measure size distribution of soot particles.

In this paper we have used TIRE-LII to measure size distribution of soot nanoparticles

in candle's flame, as a sooting diffusion flame. The intensity of the incident laser pulse is adjusted low enough that the maximum temperature of the soot particles is less than 3400 K and, consequently, one can assume low fluence LII. Therefore, sublimation term in energy equation, and mass reduction of soot nanoparticles resulting from sublimation could be ignored [9].

Furthermore, we have assumed particles to be polydisperse and to present lognormal distribution. Then, by using Levenberg-Marquaret algorithm and matching experimental data with those obtained numerically, size distribution parameters, e.g. distribution width and mean particle size have been calculated [2,10].

II. REVIEW OF THEORY AND NUMERICAL REALIZATION

Mass and energy transfer equations have been used to calculate TIRE-LII signal, emitted by soot particles heated by laser pulse, and to obtain their size distribution. Most studies on this subject are based on the model presented by Melton in 1984 who used those equations and assumed soot as spherical particles illuminated by intense laser pulses. The particles absorb laser energy, are heated up to incandescence temperature (2000-4000K) and, then, transfer energy to their environment via conduction, radiation, and sublimation. The energy balance equation is:

$$\dot{Q}_{abs} - \dot{Q}_{int} - \dot{Q}_{evap} - \dot{Q}_{cond} - \dot{Q}_{rad} = 0 \tag{1}$$

Different terms in equation (1) are explained in the following:

a. Absorption. The term $\dot{Q}_{abs}$ in Eq. 1 represents the rate of absorption of energy of laser pulse by the particles. It can be obtained by numerical calculation of Mie equations for spherical particles. In Rayleigh approximation, i.e. when $D \ll \lambda$, where D is diameter of particle, it is given by [11]:

$$\dot{Q}_{abs} = \frac{\pi^2 D^3 E(m)}{\lambda} F(t) \tag{2}$$

In Eq. 2 $F(t)$ and λ are time evolution and wavelength of the laser pulse, respectively, and $E(m)$ is absorption function of soot particle.

b. Internal energy. The term in Eq. 1, $\dot{Q}_{int}$ represents variation of internal energy of the particle and is given by [11]:

$$\dot{Q}_{int} = Mc_s \frac{dT}{dt} \tag{3}$$

where $T(t)$ is temperature of the particle at time t, M is mass of the particle, c_s is time dependent heat capacitance that is equal to [11]:

$$C_s = 28.58 + 3.77 \times 10^{-3} T - \frac{5 \times 10^4}{T^2} \tag{4}$$

c. Evaporation. $\dot{Q}_{evap}$, is energy loss due to sublimation of soot particles. If the energy of the laser pulse is so high that the maximum temperature of the particles exceeds 3400 K, soot fragments are evaporated from the surface. Energy loss due to sublimation is given by [11]:

$$\dot{Q}_{evap} = -\frac{\Delta H_V}{W_V} \frac{dM}{dt} \tag{5}$$

where ΔH_V and W_V are enthalpy and molar mass of sublimated soot particle, respectively, and dM / dt is the rate of mass depletion.

On the other hand, mass balance equation is given by [11]:

$$J_{evap} = \frac{dm_P}{dt} = -\pi D^2 N_V \frac{M_V}{N_A} \tag{6}$$

where J_{evap}, N_A, and M_V are sublimated mass flux, Avogadro constant, and sublimated molar mass respectively. In low fluence regime, sublimation term and, consequently, mass depletion of soot particles, could be neglected.

d. Conduction. The term $\dot{Q}_{cond}$ in Eq. 1 represents energy dissipation via conduction to environment gases. For atmospheric flames we assume free molecular regime ($K_n \gg 1$, where K_n is Knudsen number). In this regime, the conduction is dominated by particle-molecule collisions where the rate of energy dissipation is given by [12]:

$$\dot{Q}_{cond} = \frac{\pi D^2 \alpha_T P_0}{2T_0} \sqrt{\frac{R_m T_0}{2\pi W_a}} \left(\frac{\gamma+1}{\gamma-1}\right)(T-T_0) \qquad (7)$$

In Eq. 7 γ, P_0 and T_0 are heat capacity ratio, pressure, and temperature of the surrounding gas, respectively, α_T is thermal accommodation coefficient, R_m is universal gas constant, and W_a is molecular mass of the surrounding gas.

e. Radiation. The last term on the left hand side of Eq. 1, $\dot{Q}_{rad}$, presents energy dissipation due to radiation over all wavelengths. Using Stephan-Boltzman law this term is obtained as [11]:

$$\dot{Q}_{rad} = \pi D^2 \varepsilon \sigma_{SB}(T^4 - T_0^4) \qquad (8)$$

where γ is Stephan-Boltzman constant and ε is emissivity coefficient, that is equal to unity and 0.95 for black body and soot particles, respectively.

Using Plank distribution function for black body radiation and solving mass and energy balance equations, intensity of LII signal for a monodisperse system consisting of collection of particles with diameter, r, is obtained as [11]:

$$R(r,t) = \int_{\lambda_1}^{\lambda_2} \frac{\frac{2\pi^2 hc^2}{\lambda^5} \dot{Q}_{abs}(\lambda,r)\left(\frac{r}{2}\right)^2}{\left[\exp\left(\frac{hc}{\lambda k_B T(t)}\right)-1\right]} d\lambda \qquad (9)$$

The integration is over band pass spectrum of the filter used in the experiment. On the other hand, experimental analysis of the soot particles of atmospheric flames by using Transmission Electron Microscopy (TEM) has revealed that soot particles have different radii with lognormal size distribution function as [2, 10]:

$$P(r) = \frac{1}{\sqrt{2\pi}\sigma r} \exp\left\{-\frac{(\ln r - \ln r_m)^2}{2\sigma^2}\right\} \qquad (10)$$

where σ is distribution width and r_m is mean size of soot particles. Using of Eqs. (9) and (10), intensity of LII signal for an ensemble of polydisperse particles is obtained as [10]:

$$J(t) = \int_0^\infty N_T P(r) R(r,t) dr \qquad (11)$$

Next, we define the following parameter, which should be minimized in order to calculate distribution width and mean size of soot particles [4]:

$$\chi^2 = \sum_{i=1}^N (S_{exp}(i) - S_{theo}(i,\sigma,r_m))^2 \qquad (12)$$

where $S_{exp}(i)$ and $S_{theo}(i,\sigma,r_m)$ are experimental and numerical values of LII signal at time t_i, respectively. Levenberg-Marquart nonlinear regression algorithm has been used to minimize χ^2, and to find the best fit of numerical and experimental data. That determines values distribution width, σ, and mean particle size, r_m.

III. EXPERIMENTAL VERIFICATION

Time resolved LII technique has been used to measure emitted signal from candle's flame. Schematic of experimental setup is shown in Fig. 1.
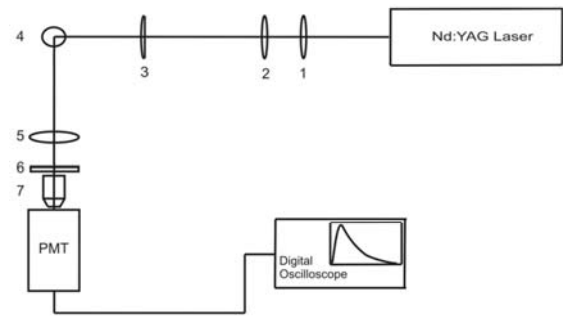
Fig. 1 Schematic of experimental setup, 1, 2: spherical lens, 3: cylindrical lens, 4: candle's flame, 5: spherical lens, 6: band pass filter, 7: objective lens.

Soot nanoparticles of the flame have been heated to temperature as high as 3000 K by pulses from a Nd:YAG laser (Ekspla NL301G, λ=1064nm, 10Hz, E= 0.6mJ/pulse, pulse duration=80ns). The output beam of the laser is first maginfied and then, using a cylindrical lens with focal length of 300 mm, has been focused on the upper part of the flame. The part of LII signal that is emitted perpendicular to direction of the laser beam has been imaged by

a spherical lens with focal length of 140 mm and diameter of 70 mm on an objective lens that focuses it on a PMT (Hamamatsu,. R329-02.). Output signal of PMT has been averaged over 500 signals and saved by using a fast oscilloscope (500 MHz, 5Gs/s). A bandpass filter with central wavelength of 455 nm and bandwidth of 10 nm (FWHM) has been used to elliminate background noise and to increase signal to noise ratio.

Initial temperature of the soot nanoparticles has been measured by a digital thermometer and is equal to 1123 K.

IV.   RESULTS AND DISCUSSION

Depending on the fluence of the laser pulse and, therefore, the maximum temperature of the soot particles, low or high fluence LII regimes may govern. In this experiment we have adjusted laser energy to satisfy low fluence regime. To verify validity of this assumption, energy balance equation is numerically solved for laser energy of 0.1 J/cm^2, initial temperature of 1123 K (that is measured by digital thermometer), and for different sizes of soot nanoparticles, i.e. 10, 70, 200, and 500 nm, and temporal evolution of their temperature has been calculated (Fig. 2).

The figure shows that the maximum temperature acquired by larger nanoparticles is higher compared to smaller particles while their rate of temperature reduction is slower. This is because for larger particles the surface to volume ratio is smaller and, therefore, heat transfer rate decreases for those particles. The results of Fig. 2 also prove that, using such level of laser energy, maximum temperature of the soot particles is less than 3400 K. Therefore, with good approximation, we can assume low fluence regime, neglecting sublimation term in balance energy equation and, therefore, the mass reduction of nanoparticles are not taken into account.
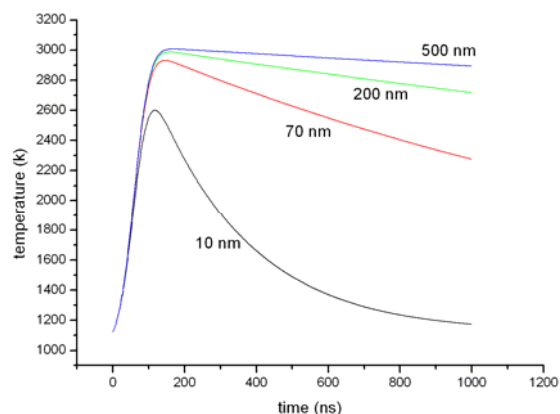
Fig. 2 Variation of temperature vs. time for soot nanoparticles of different sizes.

Figure 3 illustrates a typical experimentally measured LII signal acquired from soot nanoparticles of candle's flame illuminated by laser pulses with energy of 0.1 J/cm^2. At early stage of laser illumination the nanoparticles absorb laser energy and their temperature increase up to a maximum. Then, the particles dissipate energy in time interval on order of one microsecond, via radiation and conduction, and their temperature reduces.

On the other hand, temporal evolution of soot particle's temperature has been calculated by using mass and energy balance equations. Next, using Eqs. 9, 10, and 11, variation of LII signal, $S_{theo}(i, \sigma, r_m)$, vs. mean particle size and distribution width has been numerically calculated. Then using experimentally measured signal, averaged over 500 signals, numerically calculated signal, and Levenberg-Marquart nonlinear regression, variation of χ^2 vs. mean particle size and distribution width have been calculated (Fig. 4).
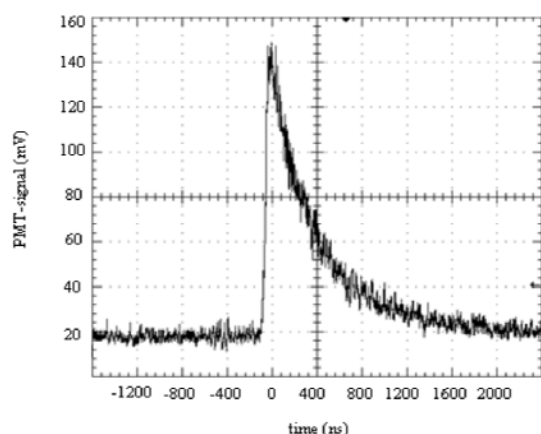
Fig. 3 Experimentally measured LII signal emitted by soot particles illuminated by laser pulses with fluence of 0.1 J/cm².

This figure shows there exists a unique point (filled circle in Fig. 4) with optimum values of the last two parameters where χ^2 is minimized. For that point, the experimental and numerical LII signals are best fitted to each others (Fig. 5). Using this method, the distribution width for lognormal distribution has been obtained to be equal to $\sigma = 0.34$ and mean particle size has been determined to be $r_m = 55\,nm$.
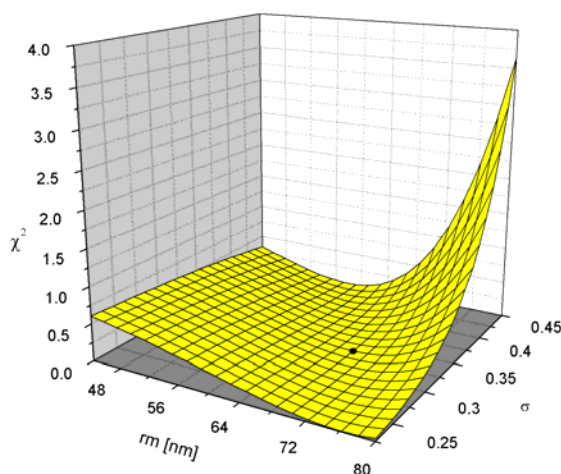
Fig. 4 Variation of χ^2 vs. mean particle size and distribution width.
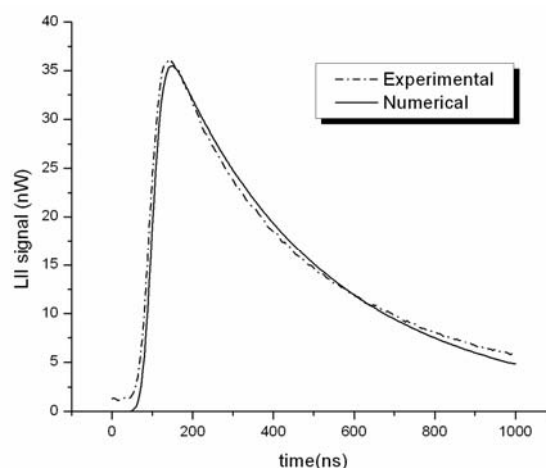
Fig. 5 Time variation of experimental LII signal (dotted line) and numerical LII signal for optimized parameters (solid line).

V. CONCLUSION

Size distribution of soot nanoparticles of candle's flame has been obtained both experimentally and numerically. To model LII signal, assuming Plank function for blackbody radiation, mass and energy balance equations have been calculated by using lognormal distribution function. Using multi dimensional nonlinear regression, distribution width and mean particle size of the soot particles have been calculated. Good agreement between numerical and experimental results is observed.

REFERENCES

[1] T. Lehre, B. Jungfleisch, R. Suntz, and H. Bockhorn, "Size distributions of nanoscale particles and gas temperatures from time resolved laser induced incandescence measurements," Appl. Opt., Vol. 42 pp. 2021-2030, 2003.

[2] L. A. Melton, "Soot diagnostics based on laser heating," Appl. Opt., Vol. 23, pp. 2201-2208, 1984.

[3] S. Dankers and A. Leipertz, "Determination of primary particle size distribution from time–resolved laser induced incandescence measurements," Appl. Opt., Vol. 43, pp. 3726-3731, 2004.

[4] R. L. Vander Wal and K. A. Jensen, "Laser induced incandescence: excitation

23

intensity," Appl. Opt., Vol. 37, pp. 1607-1616, 1998.

[5] T. Dreier, B. Bougie, N. Dam, and T. Gerber, "Modeling of time resolved laser induced incandescence transients for particle sizing in high-pressure spray combustion environments: a comparative study," Appl. Phys. B, Vol. 83, pp. 403-411, 2006.

[6] R.W. Weeks and W. W. Duley, "Aerosol particulate sizes from light emission during excitation by TEA (Transversely Excited Atmospheric pressure) carbon dioxide laser pulse," J. Appl. Phys. Vol. 45, pp. 4661-4662, 1974.

[7] S. Will, S. Scharml, and A. Leipertz, "Two dimensional soot particles sizing by time resolved laser induced incandescence," Opt. Lett., Vol. 20, pp. 2342-2344, 1995.

[8] P. Roth and A. V. Filippov, "In situ ultrafine particle sizing by a combination of pulsed laser heat up and particle thermal emission," J. Aerosol Science, Vol. 27, pp. 95-104, 1996.

[9] F. Liu, G. J. Smallwood, and D. R. Snelling, "Effects of primary particles diameter and aggregate size distribution on the temperature of soot particles heated by pulsed lasers," J. Quantitative Spectroscopy & Radiative Transfer, Vol. 93, pp. 301-312, 2005.

[10] T. Lehre, H. Bochorn, B. Jungleisch, and R. Suntz, "Development of measuring technique for simultaneous in situ detection of nanoscale particle size distributions and gas temperatures," Chemosphere, Vol. 51, pp. 1055-1061, 2003.

[11] H. A. Michelsen, F. Liu, and B.F. Kock, "Modeling Laser-induced incandescence of soot: a summary and comparison of LII models," Appl. Phys. B. Vol. 87, pp. 503-521, 2007.

[12] F. Liu, K. J. Daun, D. R. Snelling, and G. J. Smallwood, "Heat conduction from a spherical nanoparticle: Status of modeling heat conduction in laser induced incandescence," Appl. Phys. B, Vol. 83, pp. 355-382, 2006.